Evaluation and Modification of the Block Mould Casting Process Enabling the Flexible Production of Small Batches of Complex Castings

Sebastian F. Fischer and Andreas Bührig-Polaczek

Additional information is available at the end of the chapter

http://dx.doi.org/10.5772/50621

1. Introduction

In the current literature about casting processes, the block mould casting is hardly addressed although this process has numerous global applications. Almost all metallic dental implants are manufactured using this process [1-3]. This method is also regularly used in the jewellery industry [4]. The block mould casting process is particularly important for manufacturing metallic foams since it is one of the few process routes for producing cellular structures enabling uniform, open pored foams to be reproduced [5]. As the largest global producer of metallic open pored foams, the company ERG also uses the block mould casting process but rarely communicates details of the casting process. Due to the high degree of freedom the block mould casting process is very suitable for the production of bio-inspired technical devices [6].

The broad objective of this chapter consists of markedly shifting the focus of designers and manufacturers of castings to the block mould casting process. In conjunction with Rapid-Prototyping patterns, this casting method enables extremely complex castings to be variably and flexibly manufactured to their final near net shape [1, 7, 8]. A definite structuring of the pattern's surface is transferred to the casting's surface as a consequence of this method's very accurate reproduction whereby flows around the casting can be optimised in a functionally integrated way [4, 9].

Moreover, this chapter should provide the user with the possibility of optimising the block mould casting process with the aid of the depicted test results. As a consequence of the firing process, cracks can be initiated in the mould by means of which casting defects occur to the point of mould leakage. By means of optimising the mould material's water content and

temperature, the mixing duration, the firing temperature and also by adding supplements, the tendency for mould cracking is minimised by using consummate mould material manufacturing. Tests to elevate the cooling rates of the block mould casting process provide improvements in the mechanical properties of the cast metallic components.

2. State of the art

2.1. Classification of the Block Mould Casting Processes

The block mould casting process ranks among the precision casting methods in which the better known investment casting is also included. This is probably the reason why it is frequently misleadingly referred to in the literature as investment casting process. These two methods both employ the lost pattern technique. The patterns are either melted or burnt out of the mould after the moulding material has cured and are thus subsequently no longer available for mould manufacturing [1, 7, 10]. This contrasts with, for example, the widely used sand casting process, in which multiple use patterns are employed. These patterns are parted in order that they can again be used after forming the positive impression in the sand mould. Since the patterns of precision casting methods are removed from the mould by means of melting or vaporising, they do not have to exhibit mould parting. Owing to this, very complex, final near net shaped casting geometries can also be produced which possess undercuts. Apart from these advantages, precision castings exhibit a very low surface roughness compared to sand cast components which can also considerably reduced the castings' machining [4]. The difference between investment and block mould casting processes arises in the moulding material used and therefore on the mould. The patterns for the investment casting process are dipped into a ceramic slurry and subsequently sanded using ceramic granules. After the slurry has dried, this procedure is repeated until up to approx. 8 to 13 layers exist on the pattern. To manufacture a block mould, the pattern is directly embedded in a ceramic slurry where gypsum- or phosphor-bonded investments are mainly employed as the mould material [1, 11]. Thus in comparison to the investment casting process, a great deal of process time and expenditure can be saved during the block mould casting process. In addition to this, the block mould's castings are easier to demould.

2.2. Process Steps

Figure 1a) schematically depicts the sequences of the block mould casting process. The elements of the pattern are produced by injecting wax into a matrix, usually made of aluminium or steel, and are soldered with the help of bee-glue. Depending on the component to be cast, a wax base or a plate is soldered at a wax chute. If a large number of small castings are to be produced, it is sensible to fasten the patterns of the castings onto a wax base. For the production of larger castings or metal foams, a wax plate is suggested since boxes of perforated steel cuvettes are used. This cuvette stabilises the ceramic moulding material, especially during the firing process. Without this reinforcement, the mould would be damaged because of phase transitions in the moulding material which occur during firing (figure 1b).
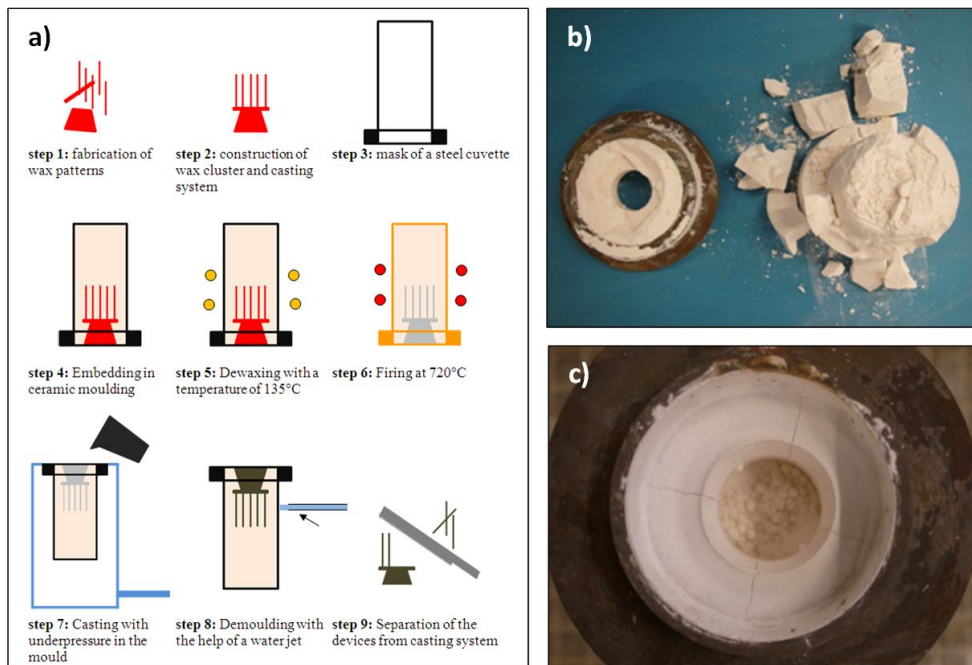
Figure 1. a) Basic steps of the block mould casting process. b) Fired block mould without stabilising cuvette. c) Block mould with cracks after the firing process.

The perforated steel cuvette is masked by plastic foil; the base is closed by a rubber plug. The inner area of the plug is filled with liquid wax via the steel cuvette and the soldered wax cluster is fixed in it. After the solidification of the fixing wax, the steel cuvette is filled with liquid ceramic slurry. The mixing of the moulding material and the filling of the steel cuvette should be carried out inside a vacuum chamber to lower the gas content in the slurry. The gas would otherwise precipitate during the moulding material's setting and lower the strength of the block casting mould. In addition to this, the surface quality of the casting will be reduced [12, 13]. The gas can also be removed from the gypsum by applying a vacuum to the moulds for some minutes after they have been filled with the slurry. In this case, the vacuum treatment should be completed prior to the start of the moulding material's setting process. After a drying period, which depends on the moulding materialused, the block casting moulds are usually dewaxed in an oven at 110 °C to 150 °C. When the moulds are completely dewaxed, the firing process is started in which heating and holding steps are adapted to the moulding material used to prevent cracking due to a too rapid heating rate. After completion of the firing process, the casting temperature is adjusted and held for at least three to four hours. Depending on the fineness of the component to be cast, a vacuum can be generated in the mould to assist the mould filling capacity of the melt (step 7, figure

1). In this way, component cross-sections smaller than 500 μm can be filled such as those which exist in, for example, open-pored metallic foams [11].

Another possibility for supporting the mould filling is to centrifugally load the block mould during the casting process. By maintaining the mould's rotational speed during the solidification phase, this also expedites the supply and the deposition of gases and impurities at the interface between the mould and the casting [1, 2]. After the mould has cooled down, the casting can be recovered by water jet or mould solving agents and removal from the casting system by a saw.

The quality of the mould, and therefore that of the casting, is decisively determined by the moulding material's mixing and by the firing process (steps 4 and 6, figure 1a). The mould tends to form cracks (figure 1c) during the firing process which can produce casting defects [3, 4, 14]. As a worst case, the liquid metal does not remain within the cavity but runs out of the mould through the cracks. In order to minimise the tendency for the block casting mould to crack, the moulding material's manufacture is generally optimised with respect to the water's temperature and quantity, mixing duration and the addition of supplements.

Since ceramic moulding compounds result in low cooling rates during solidification, it is, moreover, expedient to implement measures to elevate the cooling effect of the block mould in order to improve the mechanical properties of the metallic components since these are closely connected with the casting's cooling conditions.

2.3. Moulding and Casting Materials

A basic dilemma arises when a moulding material used in the lost mould process is chosen and prepared. The moulding material should exhibit a certain strain to withstand the load during the mould's handling, thermal stresses and the load due to the casting process. After the mould has cooled down it should also exhibit low strength in order to easily remove the casting from the mould [3, 14].

Besides these basic aspects, other requirements are imposed on the moulding materials for the block mould casting process [15]:

- flowability for good mould fillingprior to setting
- high reproductive accuracy
- fixation of the pattern
- low affinity to volume changes during the setting and firing processes
- no chemical reaction with the used casting material
- thermal stability
- short processing time
- cost-effective
- ecologically compatible

Block mould castings process's moulding materials consist of a refractory material, usually quartz, cristobalite, or a mixture of both, and a binder whereby gypsum, phosphate, metallic oxides or silicates are used. The choice of the moulding material for producing a block casting mould mainly results from the casting temperature of the material which has to be cast [16].

For aluminium and silver alloys as well as nickel-chrome alloys, a moulding material with 25 to 30 wt.% gypsum and 70 to 75 wt.% silicon oxide is used because gypsum-boned investments (GBI) exhibit good ability to collapse after casting [17].

In the past, the gypsum-bonded moulding material consists of a mixture of silica and plaster of Paris. Over the last few decades, this material has been modified by the addition of boric acid, pigments and reducing agents to, among other things, increase the strength [14]. Gypsum is produced from the sedimentary gypsum rock, whose prismatic crystals are bonded by water molecules. By treating in an autoclave, the gypsum is transformed into the unstable hemihydrate state, which needs water to restore the natural dehydrate state. When the GBI is mixed with water, branched gypsum crystals are formed which bond the refractory of the moulding material [4].

Although different statements are made in literatureabout the thermal stability of the binder, experts and producers of GBI agree that the gypsum's decomposition does not start in the temperature interval of 650 °C to 700 °C, which are common maximum firing temperatures for GBI [18, 19]. The GBI moulds should not be heated above 700 °C to 750 °C because the residual carbon from the pattern's wax then reacts with the gypsum from the moulding material. This reaction results in sulphur dioxide which decreases the surface quality of castings and,in the case of gold components, the mechanical properties [19].

High melting point alloys are cast in phosphate-bonded investments (PBI) consisting of 75 wt.% to 90 wt.% silica (quartz or cristobalite) and magnesium- or ammonium-magnesium-phosphate. This phosphate is formed by the reaction of magnesium with monoammonium in water during the mixing process. The firing process causes water loss, crystallisation and recrystallisation of magnesium phosphates, and forms fused glass, which lends high strength to PBI block casting moulds [12, 16].

The high strength of block casting moulds in the green and fired states is the biggest advantage of PBIs. At high temperatures, the strength and surface quality of the moulds are decreased due to a thermal decomposition of the binder, especially at casting temperatures above 1375 °C [14, 16].

Phosphate-bonded moulding materials are used for a broad spectrum of materials, e. g. gold, titanium, nickel, chrome and cobalt-chrome-alloys [20, 21].

The strength of gypsum or phosphate-bonded block casting moulds depends on a multiplicity of influencing factors, such as the binder, additives, storing and setting environment as well as the firing temperature. It has to be taken into account, that porosity in the ligated moulding material considerably influences the strength of the polycrystalline brittle block casting mould [14, 21]

2.4. Aspects

The block mould casting process exhibits several advantages which, when combined, cannot be found in other casting processes. Using the lost patterns casting process, ambitious geometries possessing undercuts can be realised with high dimensional accuracy, reproductive ability, and surface quality resulting in little finishing effort. The finished casting surface quality depends on the surface energy of the melt and on the interface energy between the melt and moulding materials. In this context, the composition and the purity of the melt as well as the reaction of the melt with the furnace chamber's atmosphere and the moulding material is important [17].

In conjunction with rapid-prototyped patterns the block mould casting process enables real-time production of metallic prototypes or small batches of castings. Using the ideal moulding material, nearly all casting materials can be processed using this casting method, whereby the process time is much shorter compared to the more time-consuming investment casting process [6, 8, 22, 23].

On utilising gypsum or phosphate-bonded investments, process specific disadvantages result. The GBIs or PBIs have not until now been in continuous use. This raises the price of the moulding material and limits the economic batch size at around 1,500 castings, depending on the size and geometry of the components [23]. Prior to their mixing with water, the moulding material exists as a powder, which promotes exposureto health problems in the workplace. The moulds of the block mould casting process exhibit low heat conductivity and high heat capacity. For this reason, the current cooling rate is low whichresults in unfavourable casting characteristics and low mechanical properties. Subsequent to their firing, block moulds exhibit a lower strength compared with other moulding materials. This limits the casting weight to approximately 10 kg. In addition to this, their low strength can lead to cracks in the moulds, decreasing the quality of the castings [23]. Regarding the economy of the block mould casting process, it can be concluded that this casting process is the more economical the more complex the geometry is and the smaller the dimensions of the potential cast components are.

3. Influence of sodium chloride and sodium fluoride on gypsum-bonded investment's green and fired strengths

The tendency of block moulds to form cracks has to be reduced to increase the casting component's quality (see chapter 2.2). This can be achieved by optimising the moulding material's processing and the firing process by using additives. A typical additive is sodium chloride to lower the thermal expansion of the moulding material [24]. Information is rarely given about the general effect of sodium chloride on the GBI's compressive strength, and especially about the interaction of the sodium chloride and sodium fluoride. Owing to this, the effect of sodium chloride and sodium fluoride on the strength of a GBI after firing was investigatedin the following sections.

3.1. Materials and methods

For the examinations, GBI specimen were produced containing 1 wt.%, 3 wt.% and 5 wt.% commercial table salt (based on the weight of the mixing water) with and without sodium fluoride. Higher salt contents were not used because they lead to foaming of the GBI, which decrease the handling of this moulding material. As a reference, GBI specimens without salt and only with sodium chloride were produced, respectively. The dimensions of the specimens conformed to the specifications in DIN EN 993-5. To produce the specimens, a silicon matrix was used. The particular amount of salt was dissolved in the mixing water for one minute prior to beginning the mixing process. After adding the moulding material, Goldstar xXx from Goldstarpowders (see table 1and figure 2 for the chemical composition), to the water, the composition was mixed for three minutes and then poured into the silicon matrix.

constituent	SiO2	Al2O3	Fe2O3	TiO2	CaO	K2O	P2O5	SO3	SrO	glowing loss
value [%]	75.27	0.74	0.04	0.03	10.22	0.02	0.01	13.62	0.05	3.94

Table 1. X-ray fluorescence spectroscopy results of the used GBI Goldstar xXx from Goldstarpowders.
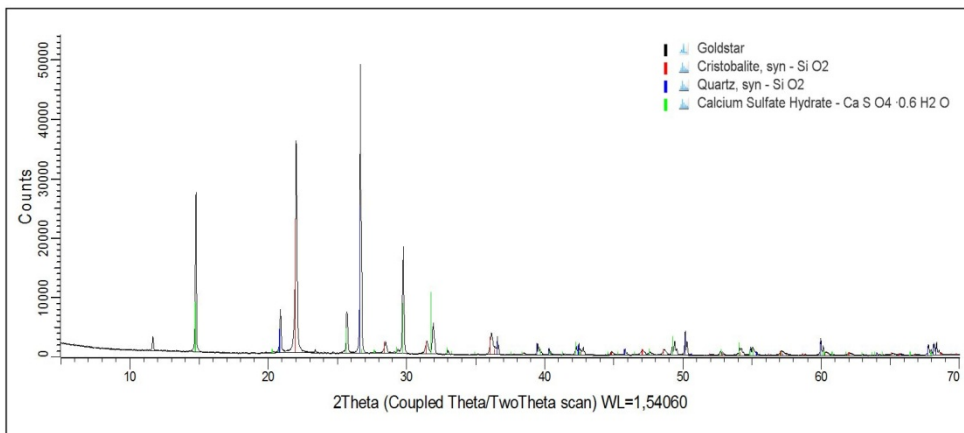

Figure 2. X-ray diffraction analysis of the used GBI Goldstar xXx from Goldstarpowders.

|					
temperature	[°C]	135	135	720	720
acceleration time	[min]	60	---	390	---
holding time	[min]	---	180	---	240

Table 2. Furnace program of the firing program.

45 Minutes after the pouring, the specimens were removed and were fired after an additional 60 minutes. The furnace program was identical to that used for the dewaxing and firing of block moulds made from the same GBI (table 2). The fired specimens were compressed using an Instron 8033 testing machine at a cross head speed of 2 mm/ min. At least four specimens were tested for each test run.

3.2. Experimental results

The influence of sodium chloride and sodium fluoride is shown in figure 3. GBI specimens with 1 wt.% sodium chloride and without fluoride have an increased compressive strength by up to 10 % in comparison with the GBI specimen without additives. With a 1 wt.% mixture of sodium chloride and sodium fluoride, the strength can be increased by about 55 %.

With the addition of these two salts, the gypsum binder reacts with sodium chloride and sodium fluoride according to the following equations [25]:

$$CaSO_4 + 2\ NaCl = CaCl_2 + Na_2SO_4$$

$$CaSO_4 + 2\ NaF = CaF2 + Na_2SO_4$$
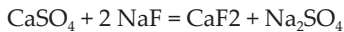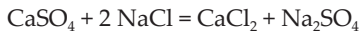
Because the strength in the green state of the GBI cannot be increased by a salt addition (see chapter 4), it is assumed that the effect can be attributed to the influence of the salt on the formation of sinter phases during the firing process. The decrease in strength can be explained by the increased setting time, which can be observed when GBI has a high salt content [26]. With an increased setting time, the gypsum dendrites start to coarsen due to the Ostwald maturation. This causes lesser cross-linking of the gypsum crystals. The effect of sodium fluoride cannot be explained by means of data in the literature.
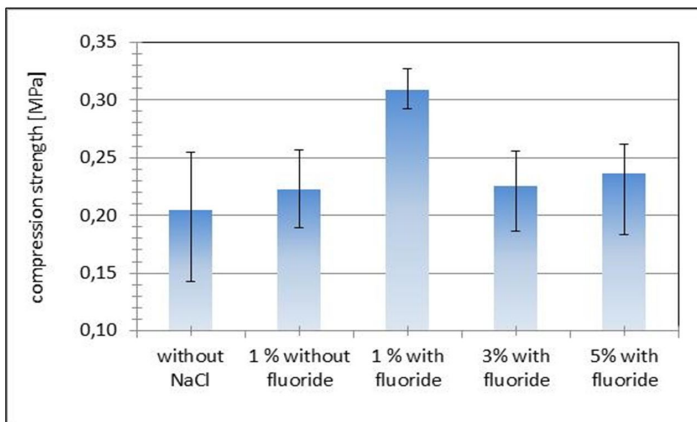

Figure 3. Influence of sodium fluoride and sodium chloride content on the gypsum-bonded investment's compression strength.

4. Influence of water temperature and content, mixing duration and quantity of salt with fluoride on the gypsum's compression strength in its green and its fired states

The quality of castings processed with the help of the block mould casting process depends to large extent on the quality of the block mould it self (see chapter 2.2 and 2.3). It is only possible to produce defect-free casting structures when the block mould exhibits strength adequate to withstand the crack initiation during the mould's production. To improve de-moulding of the casting with the help of water, the moulding material should show a low green strength after casting. For this purpose, the experiments in this section were conducted to optimise the strength of the used GBI.

4.1. Materials and methods

4.1.1. Experimental design

The experiments focused on the effect of the water temperature, water content, mixing time and salt addition (sodium chloride + sodium fluoride) on the green strength and strength of a GBI. The experiments were conducted with the help of Taguchi's method. This method covers the design of experiments according to statistical aspects, the assembling of models as well as the optimisation of the process. With the help of Taguchi arrays, only a few measurements are necessary compared to a complete factorial design. To determine the effect of the focused parameters, a L9 orthogonal array was chosen. This array allows the monitoring of 4 parameters with 3 settings, to detect non-linear relationships. Each parameter exhibits two degrees of freedom with three possible settings. These lead to a total of eight [= 4 x (3-1)] degrees of freedom. This number agrees with the demand of Taguchi that the total degree of freedom of the chosen array should be larger or equal to the number of total degrees of freedom for all experiments. In table 3, the L9 array is shown with the particular test settings.

test run	water temperature [°C] (A)	water content [%] (B)	mixing time [s] (C)	salt content [%] (D)
1	1	1	1	1
2	1	2	2	2
3	1	3	3	3
4	2	1	2	3
5	2	2	3	1
6	2	3	1	2
7	3	1	3	2
8	3	2	1	3
9	3	3	2	1

Table 3. Orthogonal L9 Taguchi array.

The settings of the water, water content and mixing time parameters were specified with the help of the literature and the specifications of the GBI manufacturer. With the help of the results from chapter 3, the salt content (sodium chloride + sodium fluoride) was determined. Table 4 summarises the settings of the parameters. If the experiments were to be conducted with the help of a complete factorial array $3^4 = 81$ test runs would have to be performed.

setting	water temperature [°C]	water content [wt.%]	mixing duration [s]	salt content [wt.%]
minimum (1)	17	45	120	0
mean (2)	35	50	180	0.5
maximum (3)	55	55	240	1.0

Table 4. Parameter settings of the experiments.

The test runs are interpreted with the aid of the analysis of means (ANOM) and the analysis of variance (ANOVA). The ANOM shows the optimisation direction of the factors. The mean deviance from the total average caused by every factor level indicates the main effect of every single factor level [27, 28]:

$$\bar{\eta}_{A1} = \frac{1}{n}[(\eta_{11} + \eta_{12} + \eta_{13}) + (\eta_{21} + \eta_{22} + \eta_{23}) + (\eta_{31} + \eta_{32} + \eta_{33})] \tag{1}$$

$$\bar{\eta}_{A2} = \frac{1}{n}[(\eta_{41} + \eta_{42} + \eta_{43}) + (\eta_{51} + \eta_{52} + \eta_{53}) + (\eta_{61} + \eta_{62} + \eta_{63})] \tag{2}$$

$$\bar{\eta}_{A1} = \frac{1}{n}[(\eta_{71} + \eta_{72} + \eta_{73}) + (\eta_{81} + \eta_{82} + \eta_{83}) + (\eta_{91} + \eta_{92} + \eta_{93})] \tag{3}$$

$\bar{\eta}_{ij}$ are the measured values and n is the total number of all trials (for $L_9 = 9$).

The effects E of the level changing are for the factor A:

$E_{A1,2} = \bar{\eta}_{A2} - \bar{\eta}_{A1}$ and $E_{A1,3} = \bar{\eta}_{A3} - \bar{\eta}_{A1}$

With the aid of the ANOVA, the statistical significance of an effect of a parameter on the command variable can be evaluated. For this, the total result is partitioned into single variances. The variance expresses the squared deviance of the particular average.

The calculation of the ANOVA is performed with the help of the following equations [27, 28]:

I.   Calculation of a correction factor (CF) for an easier calculation of the error:

$$SS_m = \frac{\left(\sum \eta_{ij}\right)^2}{N} = CF \tag{4}$$

N is the number of all trials including all repeatings (L9 array with three repeatings per trial → N = 9 x 3 = 27)

II. Calculation of the total sum of squares

$$SS_{total} = \sum \eta_{ij}^2 - CF \tag{5}$$

III. After this the sum of the squared deviances of every factors is built, here exemplary for factor A:

$$SS_A = \frac{\left(\sum \bar{\eta}_{A1}\right)^2}{N_{A1}} + \frac{\left(\sum \bar{\eta}_{A2}\right)^2}{N_{A2}} + \frac{\left(\sum \bar{\eta}_{A2}\right)^2}{N_{A3}} - CF \tag{6}$$

N_{A1}, N_{A2}, N_{A3} are the number of trials with the parameter on level 1, 2 or 3.

IV. Error sum of squares

$$SS_{error} = SS_{total} - \left(SS_A + SS_B + SS_C + SS_D\right) \tag{7}$$

V. Degrees of freedom (f_{total} and $f_{parameter}$)

$$f_{total} = \text{total number of trials} - 1 \tag{8}$$

$$f_A = \text{number of levels of parameter A} - 1 = 3 - 1 = 2 \tag{9}$$

VI. For the evaluation of the variances for each factor (for example A)

$$V_A = \frac{SS_A}{f_A} \tag{10}$$

$$V_{error} = \frac{SS_{error}}{f_{error}} \tag{11}$$

VI. Calculation of the ratio of the variance and the error variance (for example A)

$$F_A = \frac{V_A}{V_{error}} \tag{12}$$

VIII. Verifying the significance of the factors with the help of the F-Test. For this the calculated F value is compared with a tabulated F value. If the calculated one is bigger, the observed result is statistical significant.

Within the Taguchi method the signal to noise ratio (S/N) represents the summed statistic. For this, every measured value of every test run is reweighted in a target function such that no repetition within one test run occurs and that the total degree of freedom is decreased. There are different target functions which can be chosen for the S/N-ratio depending on the quality attribute. If the aim is to minimise the number of trials (smaller-the-better-type), the S/N-ratio is calculated in the following way [27]:

$$\eta = -10 \times \log\left(\frac{1}{n}\sum_{i=1}^{n} y_i^2\right) \tag{13}$$

The maximisation of the S/N-ratio (lager-the-better-type) is

$$\eta = -10 \times \log\left(\frac{1}{n}\sum_{i=1}^{n} \frac{1}{y_i^2}\right) \tag{14}$$

Using the S/N-values, the ANOM and the ANOVA can be calculated in the same way; similar to the mean values.

Utilising the Taguchi method in this way aims at setting a process such that the target value achieves the desired maximum or minimum with low scatter. To verify the data resulting from Taguchi experiments, one should perform verifying experiments.

The value of the command variable η_{optimal}, under optimal conditions, is calculated from the optimal parameter settings [28]:

$$\eta_{\text{optimal}} = \bar{\eta} + (\bar{\eta}_{A_i} - \bar{\eta}) + (\bar{\eta}_{B_i} - \bar{\eta}) + (\bar{\eta}_{C_i} - \bar{\eta}) + (\bar{\eta}_{D_i} - \bar{\eta}) \tag{15}$$

with $\bar{\eta}$ = overall mean of the target value

The confidence interval for the approving experiment ($CI_{\text{confirmation}}$) and of the population ($CI_{\text{population}}$) are calculated by

$$CI_{\text{confirmation}} = \sqrt{F_a(1, f_e) \times V_{\text{error}}\left[\frac{1}{n_{\text{eff}}}\right] + \left[\frac{1}{R}\right]} \tag{16}$$

$$CI_{\text{population}} = \sqrt{\frac{F_a(1, f_e) \times V_{\text{error}}}{n_{\text{eff}}}} \tag{17}$$

$$n_{\text{eff}} = \frac{N}{1 + total DOF associated in the estimate of mean} \tag{18}$$

R = sample size for confirmation experiments

$F_a(1, f_e)$ = tabulated F-value

4.1.2. Production and testing of specimens

For the production of the compression specimen the corresponding amount of GBI (Gold-star xXx from Goldstarpowders, table 1 and figure 2) was mixed with max. 825 g water with the help of a drill-stirrer. If salt was used for a test run, the salt was dissolved in the mixing water for 1 minute. After mixing, the slurry was poured in a silicon matrix to produce compression specimens according to DIN EN 993-5, and after 45 minutes the specimens were removed and fired (table 2). The compression tests were conducted using an Instron 8033 at a cross head speed of 2mm/min. For every test run, three and five specimens in the green and fired states were tested, respectively.

4.2. Experimental results

Table 5 summarises the results of the compression tests and the S/N-ratio for every test run.

test run	green strength response 1	green strength response 2	green strength response 3	green strength S/N [dB] (smaller-the-better)	strength response 1	strength response 2	strength response 3	strength response 4	strength response 5	strength S/N [dB] (larger-the-better)
1	2.42	2.40	3.00	-8.37	0.20	0.24	0.18	0.29	0.21	-13.33
2	1.89	1.70	1.70	-4.93	0.24	0.22	0.25	0.34	0.24	-12.04
3	1.17	1.11	1.10	-1.03	0.25	0.23	0.24	0.31	0.24	-12.04
4	2.28	1.66	2.13	-6.19	0.38	0.51	0.37	0.40	0.51	-7.50
5	2.44	2.76	2.25	-7.93	0.20	0.24	0.20	0.22	0.21	-13.45
6	1.42	1.58	1.65	-3.82	0.18	0.16	0.16	0.16	0.18	-15.53
7	2.11	2.18	2.16	-6.64	0.20	0.23	0.24	0.22	0.21	-13.20
8	1.46	1.38	1.64	-3.50	0.25	0.23	0.27	0.26	0.24	-12.08
9	2.03	2.12	2.06	-6.32	0.18	0.18	0.20	0.20	0.13	-15.33

Table 5. Results of the compression tests and calculated S/N ratios.

The aim of the presented experiments was to maximise and minimise the GBI's strength in the fired and the green states, respectively. That is, the larger and the smaller the S/N-ratios were selected which are the better in the fired state the better in the green state, respectively.

The results of the ANOM are presented in figures 4 to 7; tables 6 and 7 present the results of the ANOVA. Figures 4a) and 5a) and table 6 show that the water temperature and the mixing time have little effect on the green compression strength of the used GBI. This contrasts

with the water and salt contents (figures 4b and 5b). From the literature, it is known that the strength of GBI decreases with increasing water content.
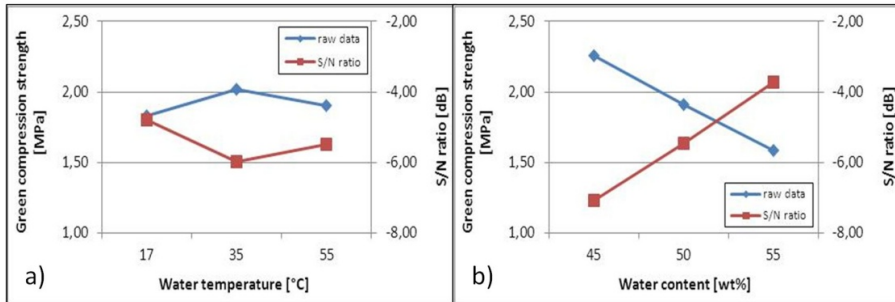

Figure 4. Influence of a) water temperature and b) water content on green compression strength of gypsum-bonded investments.

Owing to its heterogeneous nucleation, gypsum spontaneously crystallises without being in its equilibrium condition even in the first stages of the hydration process. Excess water, which is important for the flowability of the moulding material, is not bonded after the re-hydration of the gypsum and evaporates during setting leaving pores in the material. This microstructural defect considerably decreases the strength of the GBI. In addition to the pore formation, an increased water content leads to an increase in the gypsum's setting time, which produces a coarsening of the gypsum crystals due to Ostwald maturation. These crystals built a less dense network which cannot carry the magnitude of load that a better cross-linked gypsum crystal network is capable of [21, 26, 29].

On increasing the salt content from 0 wt.% to 1 wt.% severely decreases the green strength of GBI (figure 5b). An explanation of this result cannot be interpreted with the help of the literature.

In the fired state, all the varied parameters show an effect on the compression strength. The maximum strength is achieved with a mean water temperature, low water content, mean mixing time and a high salt content.

The effect of the water temperature on the GBI's compressive strength is similar in both the green and the fired states, but the impact is more pronounced in the fired state. The best water temperature for optimising the compressive strength lies in the range of 17 °C to 55 °C. A reason for this could be the change in the gypsum's solubility in water. When water reaches the temperature of approx. 27 to 35 °C, the solubility of gypsum in water is decreased resulting in a lower amount of hydrated gypsum. This gypsum is hydrated between the start of mixing and the setting. Due to this, less gypsum crystals are formed and thus the strength of the moulding material is decreased [30, 31].
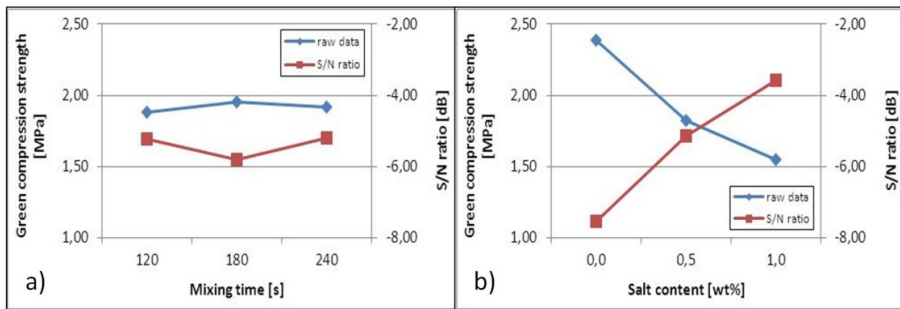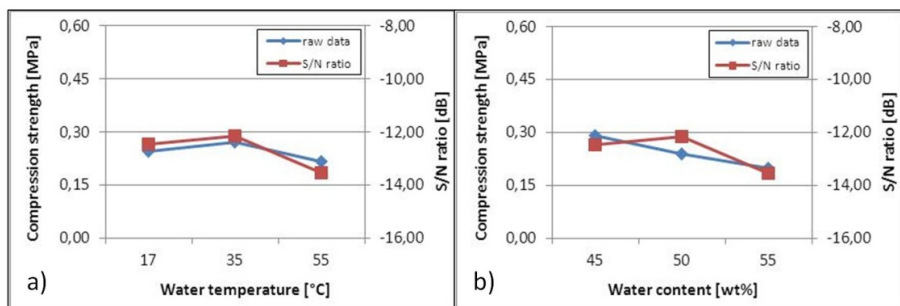
Figure 5. Influence of a) mixing time and b) salt content on green compression strength of gypsum-bonded investments.

source	SS	DOF	V	F-ratio	SS'	P (%)
water temperature [°C] (A)	0,16	2,00	0,08	pooled	---	---
water content [%] (B)	2,07	2,00	1,03	27,72	1,99	32,07
mixing time [s] (C)	0,02	2,00	0,01	pooled	---	---
salt content [%] (D)	3,29	2,00	1,65	44,17	3,22	51,82
error (pooled)	0,67	18,00	0,04	---	1,00	16,11
total (T)	6,21	26,00	---	---	6,21	100,00

Table 6. ANOVA of the green compression strength (raw data). The tabulated critical f-value is 3.55.

Figure 6. Influence of a) water temperature and b) water content on compression strength of fired gypsum-bonded investments.

In contrast to the green state, the effect of different water contents on the compression strength of GBI is minor. The effect of pores, which are built because of excess water, is lower because probably some sinter phases are formed during the firing process.
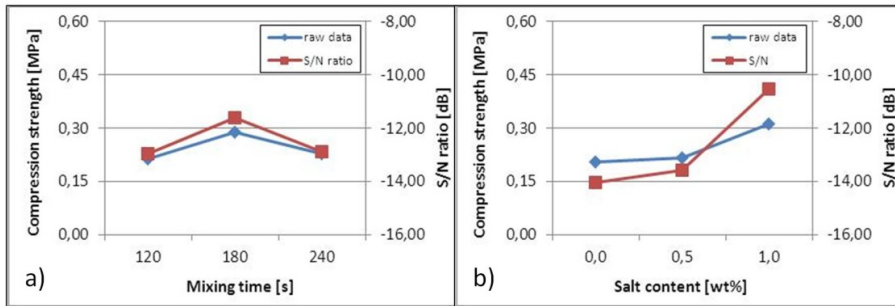
Figure 7. Influence of a) mixing time and b) salt content on compression strength of fired gypsum-bonded investments.

source	SS	DOF	V	F-ratio	P (%)
water temperature [°C] (A)	0,02	2,00	0,01	9,03	7,24
water content [%] (B)	0,06	2,00	0,03	24,83	21,49
mixing time [s] (C)	0,05	2,00	0,02	18,59	15,86
salt content [%] (D)	0,11	2,00	0,05	40,46	35,58
error (pooled)	0,05	36,00	1,30E-03	---	19,84
total (T)	0,29	44,00	---	---	100,00

Table 7. ANOVA of the compression strength (raw data). The tabulated critical f-value is 3.32.

The impact of the mixing duration on the compressive strength shows the same tendency in the green and in the fired state. The strength rises from the beginning of the mixing process up to 180 seconds. After this peak, the strength decreases with continuous mixing. 180 seconds mixing advances the hydration of the gypsum and leads to a higher strength after setting and burning, respectively, because more gypsum crystals are precipitated. However, once precipitated, the crystals are destroyed by the mixing. After mixing for the ideal duration, destruction of the crystals dominates and the resulting strength again decreases [26].

The influence of the salt content can be attributed to the formation of sinter phases during the firing process.

4.3. Confirmation tests

The specimens for the verification test runs were produced with the parameter settings summarised in table 8. In addition to this, the calculated and measured values for the reference specimens are presented.

The measured values are located within the calculated scattering bands and deviate only marginally from the calculated average values. Firstly, it can be concluded that the obtained

results have a major significance. Secondly, that there is no interaction between the parameters; otherwise the calculated values would differ more strongly from the measured results since these calculations are only based on the single effect of the parameters. It is interesting that there is no interaction between the water content and the mixing duration. Although the setting process is slowedusing increased water content, a mixing duration longer than 180 seconds in combination with high water contents has no unfavourable effect on the compressive strength of GBI after either setting or firing. Since the unfavourable effect of the mixing duration can be attributed to the destruction of gypsum crystals, it follows that, independent of the water content, a nearly equal amount of gypsum crystals are present after the mixing process.

water temperature [°C]	water content [wt.%]	mixing duration [s]	salt content [wt.%]	calculated strength [MPa]	average strength [MPa]
17	45	180	1	0,41 ± 0,07	0,40 ± 0,05

Table 8. Setting of the parameters of the confirmation tests, the calculated strength for a confidence interval of 95 % and the measured strength.

5. Influence of glass fibre volume and fibre length on the strength of fired gypsum-bonded investments

When the compositions of several GBIs are examined it can be shown that some products contain glass fibres to increase the strength of the block mould. The reinforcement of GBI and the effect of glass fibres on the properties of GBI were the focus of several examinations [32-36]. The results were contradictoryregarding the effect of the glass fibres on the compressive strength of GBI. Due to this, the aim of the following analyses was to demonstrate the influence of the glass fibre volume and glass fibre length on the compressive strength of a GBI.

5.1. Materials and methods

Uncoated short glass fibres were used. Coated glass fibres could lead to both a chemical reaction and a bond between fibres and moulding material which exerts an adverse effect on the reinforcement [32]. The maximum fibre content was held constant at 1.0 wt.% based on the weight of the moulding material. Larger amount of glass fibres could not be added because the viscosity of the slurry was otherwise too low. The mean glass fibre content was 0.5 wt.%. The glass fibre lengths employed were 3 mm, 6 mm to 12 mm. For the production of the compression specimens, 1500 g of the GBI Goldstar xXx from Goldstarpowders (composition see table 1 and figure 2) was mixed with the glass fibres and then with 675 g water for three minutes. The slurry was poured into a silicon matrix to produce compression specimens according to DIN EN 993-5. The specimens were removed and fired (table 2) after 45 minutes and 60 minutes, re-

spectively. With the help of an Instron 8033 testing machine (cross-head speed = 2mm/min), the compressive behaviour of at least four specimens were determined.

5.2. Experimental results

The results of the compression tests are shown in figure 8. In general, the reinforcement of GBI specimens using glass fibres decreases the scatter of the compression test results. The weakening effect of the pores is attenuated, which are the main reason for the deviations of the measured compressive strength, independent of the volume and length of the glass fibres.
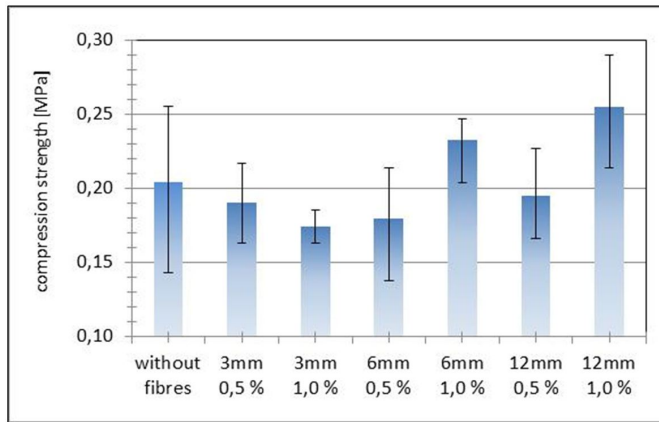
Figure 8. Influence of short fibre content and short fibre length on compression strength of fired gypsum-bonded investment.

The moulding material's compressive strength is only slightly attenuated by glass fibres with a length of 3 mm and a fibre content of 0.5 wt.%. An increase in the compressive strength of up to 25 % can be achieved by reinforcing the GBI using 1.0 wt.% of 6 mm and 12 mm glass fibres. This content and these lengths improve the resistance of the moulding material to the initiation of micro cracks and their growth. Following micro crack initiation due to loading the fibre-reinforced moulding material, the crack reaches the glass fibre and growths along the interface of the matrix and fibre; thus dissipating crack energy [32, 36].

6. Influence of metal powder in the moulding material on the GBI's setting behaviour and its compressive strength as well as on the cooling behaviour, the metallographic and mechanical properties of an A356 (AlSi7Mg0.3) alloy

Despite several advantages, the block mould casting process exhibits some unfavourable characteristics (see chapter 2.4). One of the most severe problems is the low cooling rate of

this casting process during the solidification of liquid metals. For example, this cooling rate amounts to approximately 0.1 K/s during the solidification of an A356 alloy at a casting temperature of 720 °C. In contrast to this, the high pressure die casting process with a similar alloy and wall thicknesses reaches cooling rates between 50 and 85 K/s [37]. Owing to the low heat conductivity of the moulding materials used, the cast metal solidifies relatively slowly producing a coarse microstructure and a high dendrite arm spacing (DAS). These microstructural parameters lead to decreased mechanical properties of the metallic components [23, 38]. Besides the mechanical properties, the low cooling rate impairs the casting properties. Inferior casting properties lead to technical volume deficits in the casting; such as shrinkage or microporosity. Low cooling rates induce a segregation of elements in the melt adjacent to the solidification front thus promoting constitutional undercooling. This changes the solidification morphology with a tendency to produce exogenous mushy and endogenous papescent structures. These types of solidification morphologies decrease the feeding ability of the metallic melt, from which microporosity results [39]. Methods for improving the cooling rate of the block mould casting process leads directly to an improvement in the casting and mechanical properties.

The presented trials aimed at increasing the cooling rate of the block mould casting process with the help of iron powder. Besides the iron powder affecting the cooling of the metal castings in the block moulds, the impact of the iron powder on the setting and strength of the moulding material is evaluated.

6.1. Materials and methods

To evaluate the influence of iron powder, compression specimens according to DIN EN 993-5 were produced. A specific amount of iron powder was mixed with 1500 g Goldstar xXx from Goldstarpowders (composition see table 1 and figure 2) and then introduced in 50 wt.%, 55 wt.% and 60 wt.% water. After 3 minutes mixing, the liquid moulding material was poured into a silicon matrix. After 60 minutes, the GBI specimens were removed and, following another 60 minutes, the specimens were fired (table 2). At least three specimens per test run were compression tested at a cross head speed of 2 mm/min with the aid of an Instron 8033 testing machine.

To investigate the effect of applying a vacuum, some silicon matrixes, which were filled with liquid iron powder GBI mixture, were evacuated.

The effect of the metal powder in the moulding material on the cooling behaviour of an A356 alloy was measured with the aid of thermal analyses, tensile tests and metallographic sections. To enable this, a wax assembly possessing four tensile specimen patterns was produced, whereby a type K thermocouple was integratedinto the middle of one tensile specimen per assembly. With the help of preliminary tests, a maximum (75 wt.%) and a mean (37.5 wt.%) iron powder content was specified. After embedding the patterns into the GBI (Goldstar xXx from Goldstarpowders, composition see table 1 and figure 2) mixed with iron powder, the block moulds were dewaxed, fired and cooled down to 200 °C. A pre-grain refined, not modified N-degassed A356 alloy was cast into the block moulds using a casting temperature of 720 °C. After the melts had cooled down, the tensile specimens were tested. Specimens with integrated

thermocouples were used to prepare metallographic sections. For this purpose, the corresponding samples were mounted using the embedding compound Araldit DBF together with the hardener Ren HY 956. The mounted samples were ground using different grades of abrasive paper and polished using VibroMet. Light microscopy images were taken at different magnifications using an Axio Imager A 1 m from the company Zeiss.

6.2. Experimental results

At the beginning of the investigations, it was attempted to determine the iron powder content at which the GBI would no longer set. It was possible to show that the setting process was never interrupted, irrespective of the iron powder content. Figures 9 and 10a) show the effect of metal iron powder on the setting time of the used GBI. In addition to the increase owing to a higher water content, the setting time increases with elevated iron powder content, yet the setting process is not interrupted. A reason for this cannot be found in literature.
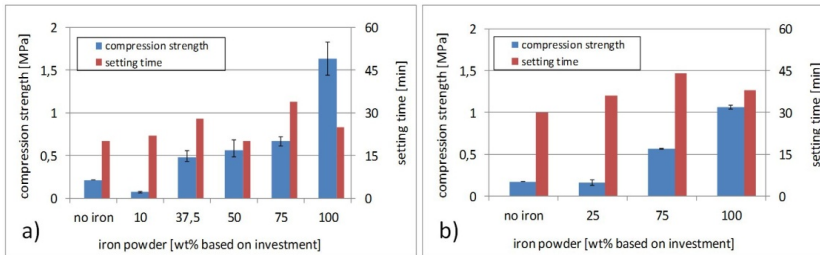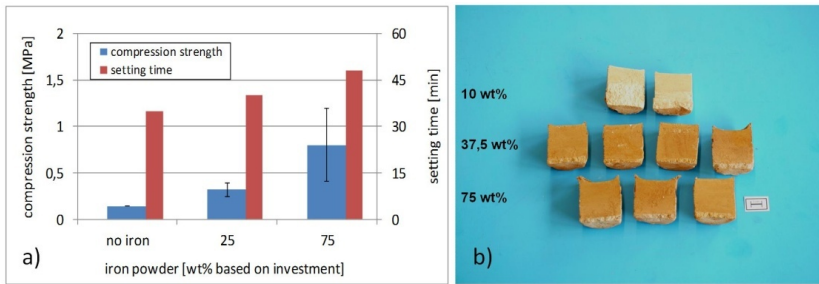

Figure 9. Influence of iron powder on the compressive strength and setting of gypsum-bonded investments with a) 55 wt.% water and b) 60 wt.% water.

Besides the setting time, the influence of the iron powder on the compressive strength of the used GBI is shown in figures 9 and 10b). From the critical value (10 wt.% to 25 wt.%), the compressive strength of the GBI is increased independent of the specimen's water content. The maximum difference in the compressive strength of specimens with 100 wt.% and without iron powder content is more than 750%. With the aid of references in the literature, it is assumed that the iron decreases the melting point of the GBI's refractory. Due to this, fewer sinter phases are formed which considerably increase the strength of the moulding material [40].

The analysis of the vacuumed GBI specimens possessing different metal powder contents indicates that the iron powder is well distributed within the fired GBI specimens (figure 10b). There is no segregation of the metal powder due to the underpressure.

Figure 11a) shows the effect of the iron powder in the moulding material on the cooling behaviour of an A356 alloy. Using the first derivative of the cooling curves, the liquidus temperature and the temperature at the end of solidification were detected. In combination with the respective times, the cooling rates achieved by the block moulds were calculated (figure 11b). The cooling rate of the block mould casting process can be increased by factor of 3.5

with the help of 37.5 wt.% iron powder in the moulding material. The addition of more iron powder exhibits no further increase.

The increased cooling rates are reflected in the dendrite arm spacing (DAS) of the A356 alloy. Owing to a 3.5 fold increase in solidification rate due to the iron powder addition, the DAS is decreased by about 33 % in comparison to specimens produced using moulds containing no iron powder (figure 11a). Since there is no changing in the amount of the cooling rate, no change in the DAS was found due to increasing the iron powder content from 37.5 wt.% to 75 wt.%.

Figure 10. a) Influence of iron powder on the compressive strength and setting of gypsum-bonded investments with 65 wt.% water. b) Influence of vacuum on the distribution of iron powder in the ceramic specimens.
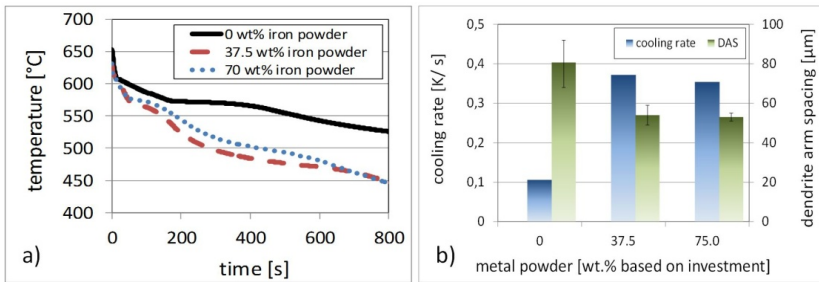

Figure 11. Influence of iron powder on the cooling rate of block moulds casted with an A356 with a casting temperature of 720 °C and a mould temperature of 200 °C. a) Cooling curves. b) Calculated cooling rates and the DAS of the specimens.

The effects of the increased cooling rate and the decreased DAS cannot be related to the mechanical properties of the A356 alloy (figure 12). According to the literature, the mechanical properties of those specimens produced with the aid of the modified moulds which promote a higher cooling rate should be better than the properties of those specimens cast using the unmodified moulds. In contrast to this, the tensile strengths and particularly the elongations to fracture of the specimens produced with the aid of the block moulds containing 37.5 wt.% iron powder are, in fact, worse compared to those of specimens cast in non-modified

moulds. The tensile strengths and elongations to fracture of specimens from modified moulds can be increased if the iron powder content is raised to 75 wt.%.

The metallographic sections of the A356 alloy specimens show that these results can be attributed to iron phases in the aluminium-silicon matrix. When the mean content of the iron powder is employed in the mould, the alloy's microstructure exhibits the most iron containing phases. It appears that during the mould filling and solidification of the A356 alloy, iron was dissolved out of the mould by the aluminium melt. The solubility of iron in solidified aluminium is low, which promotes the precipitation of the iron phases during the solidification. These plate-like phases decrease the tensile strength and the elongation to fracture and also increase the yield strength (figure 12 and figure 13c).
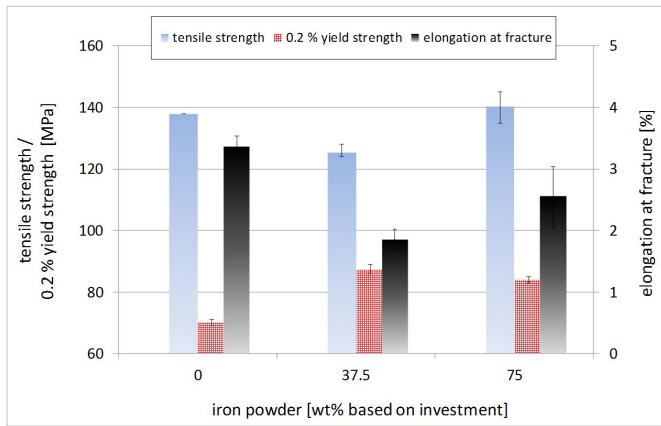

Figure 12. Influence of iron powder in the block mould on the tensile properties of an A356.
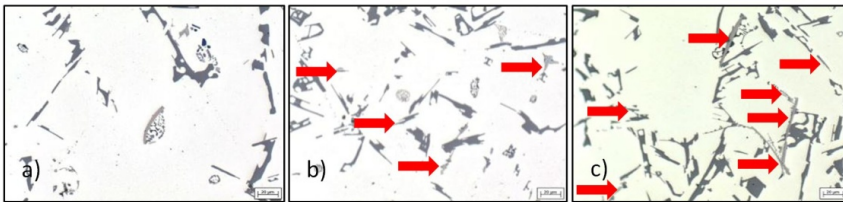

Figure 13. Metallographical sections of specimens casted in block moulds with a) 0 wt.%, b) 75 wt.% and c) 35.5 wt.% iron powder. Some iron phases are marked.

The lower yield strength and the lower fraction of iron phases in the microstructure indicate that the specimen cast in the mould containing 75 wt.% iron powder dissolved less iron in comparison to the specimen produced with the help of moulds containing 37.5 wt.% iron

powder. This assumption could be explained by the higher strength of the moulds with 75 wt.% iron powder (figure 13b), since they dissolve less iron content due to mould erosion.

7. Influence of the maximum firing temperature and duration on gypsum-bonded investment's compressive strength

During the firing process, thermal stresses develop in the block mould due to the different thermal expansion coefficients of the moulding material's constituents. For example, in GBI bonded moulds the gypsum contracts during the firing process due to dehydration and the binder decomposes at elevated temperatures [14]. The dehydration takes place at temperatures of around 128 °C whereby hemihydrate is formed, in which water is removed at 163 °C. Depending on the temperature, the resulting anhydrite exhibits three polymorphic states. At 200 °C, III-$CaSO_4$ (hexagonal) is transformed into II-$CaSO_4$ (orthorhombic). Above 1200 °C, I-CaSO4 (cubic) is formed [24]. The fireproof basic material silica, mostly a mixture of cristobalite and quartz, shows a phase transformation at 220 °C to 275 °C and 573 °C, respectively. This transformation leads to an expansion of these phases. The isotropic transformation of cristobalite from the α- to β-modification takes place rapidly and causes a shearing moment between the refractory and the binder. Moreover, this moment can induce cracks in the mould. The expansion of quartz is anisotropic and can rapidly elevate the shearing moment caused by the cristobalite [14].

Independent of the crack formation due to the refractory's expansion, cracks can be initiated in the block mould by the expansion of the wax pattern during the dewaxing process or by a too rapid cooling after firing [14].

The tendency to decrease the crack initiation directly leads to a qualitative improvement of block mould cast components. For this purpose, the firing process was modified regarding the maximum firing temperaturein the followinginvestigations.

7.1. Materials and methods

The effect of the maximum firing temperature on the strength of GBI was analysed with the help of compression tests. For this, the moulding material Goldstar xXx from Goldstarpowders (composition see table 1 and figure 2) was used to produce compression specimens accordingly to DIN EN 993-5. The mixing procedure was conducted with respect to the results in section 4. Two types of specimens were produced: One with the best and one with the worst settings for the mixing parameters (table 9).

The general furnace program is summarised in table 2 with varying maximum burning temperatures. The highest furnace temperature was fixed at 950 °C to avoid a decomposition of the gypsum [14]. The compression specimens were tested using an Instron 8033 at a cross head speed of 2mm/min.

strength	water temperature [°C]	water content [wt.%]	mixing duration [s]	salt content [wt.%]
minimum	17	55	240	0
maximum	17	45	180	1

Table 9. Mixing conditions for the production of the GBI specimens.

7.2. Experimental results

Figure 14 shows the results of the firing experiments. By increasing the maximum firing temperature up to 950 °C, the compressive strength of GBI specimens is increased independent of the starting strength. A probable reason for this is that a greater quantity of sinter phases is formedat higher firing temperature which raises the strength of the moulding material. However, the scatter of the strength values is increased with elevated firing temperatures. In addition to this, there is a large difference between the strength of specimens produced using an optimised setting of the mixing parameters and that of other specimens.
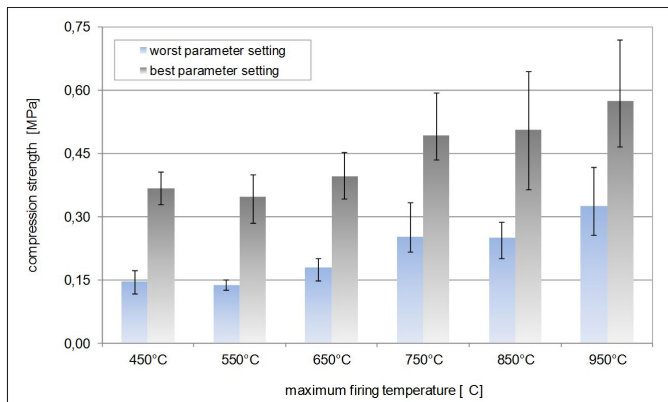

Figure 14. Influence of maximum firing temperature on the compression strength of gypsum-bonded investments.

8. Conclusions

The block mould casting process offers several attractive advantages which, when combined, only exist in this process. Besides this, high dimensional accuracy and surface quality of the potentially complicated casting result in low finishing effort. To produce high quality, block mould cast components, the tendency of the block mould to cracking has to be minimised. In the investigations presented here, different approaches were followed to modify the block moulds:

1. The addition of sodium chloride and sodium fluoride to the mixing water considerably increases the strength of the GBI block moulds. Regarding the handling of the GBI, a salt content of one weight per cent should not be exceeded.

2. In the green state, only the water and the salt content have a statistically significant influence on the strength of the GBI. Increasing the water and salt contents decreases the strength of the GBI in the green state. Here, the water temperature and the mixing duration have no significant influence.

3. The water temperature and the mixing duration exert a statistically significant effect on the fired state. The maximum strength is achieved using a water temperature of 17 °C, a low water content (here 45 wt.%), moderate mixing duration (here 180 s) and a high salt content of one weight per cent.

4. The results depicted here allow the green strength of GBI to be minimised providing a better demoulding of the block mould cast components. In addition to this, the strength in the fired state can be optimised to avoid crack initiation in the block moulds. Salt (sodium chloride + sodium fluoride) increases the green strength and decreases the fired strength.

5. One weight per cent of 12 mm glass fibres raise the strength of GBI.

6. Iron powder increases the strength and the cooling rate of GBI. Owing to the best agreement obtained between erosion resistance and cooling rate, a powder content of 75 wt. % is suggested. To avoid the assimilation of iron by the aluminium melt, coating of the wax pattern it advised.

7. With increased maximum firing temperature, the strength of GBI is raised, whereby a temperature of 950 °C should not be exceeded.

Acknowledgements

Author details

Sebastian F. Fischer[*] and Andreas Bührig-Polaczek

*Address all correspondence to: s.fischer@gi.rwth-aachen.de

Foundry-Institute, RWTH Aachen University, Aachen, Germany

References

[1] Wu, M., Tinschert, J., Augthun, M., Wagner, I., Schädlich-Stubenrauch, J., Sahm, P. R., & Spiekermann, H. (2001). Application of laser measuring, numerical simulation and rapid prototyping to titanium dental castings. *Dental Materials*, 17(2), 102-108.

[2] Lautenschläger, E. P., & Monaghan, P. (1993). Titanium and titanium alloys as dental materials. *International Dental Journal*, 43(3), 245-253.

[3] Luk, H. W. K., & Darvell, B. W. (1997). Effect of burnout temperature on strength of phosphate-bonded investments. *Journal of Dentistry*, 25(2), 153-160.

[4] Guler, K. A., & Cigdem, M. (2012). Casting Quality of Gypsum Bonded Block Investment Casting Moulds. *Advanced Materials Research*, 445, 349-354.

[5] Ashby, M. F., Evans, A., Fleck, N. A., Gibson, L. J., Hutchinson, J. W., & Wadley, H. N. G. (2000). *Metal Foams- A Design Guide*, Woburn: Butterworth-Heinemann.

[6] Fischer, S. F., Schüler, P., Bayerlein, B., Fleck, C., & Bührig-Polaczek, A. (18-21 September). Paper presented at Proceedings of 7th International Conference on Porous Metals and Metallic Foams, MetFoam11, Busan, Korea. *Some aspects of the optimisation of open-pore metal foams by introducing bio-inspired hierarchical levels. In: Hur BY, Kim SE, Hyun SK. (eds.)*, BEXCO, 57-62.

[7] Bührig-Polaczek, A., Fettweis, D., & Hett, M. (12-14 October 2004). Paper presented at Proceedings of "Cellular Metals and Polymers ", Zürich, Switzerland. *Casting of metallic sponges using rapid prototyping. In: Singer RF, Körner C, Altstädt V, Münstedt H. (eds.)*, Trans Tech Publications, 65-68.

[8] Maguire, M. C., Baldwin, M. D., & Atwood, C. L. (1995). Fastcast: Integration and application of rapid prototyping and computational simulation to investment casting. . In: Society for the advancement of materials and process engineering: proceedings of 27th International Sampe Technical Conference 9- 12 October Albuquerque, New Mexico , 27, 235-244.

[9] Ivanov, T., Bührig-Polaczek, A., & Vroomen, U. (2011). Casting of microstructured shark skin surfaces and applications on aluminium casting parts. *Foundry*, 60(3), 229-233.

[10] Veeck, S., Lee, D., & Tom, T. (2002). Titanium Investment Castings. *Advanced Materials and Processes*, 160(2), 59, 62.

[11] Fischer, S. F., Thielen, M., Loprang, R. R., Seidel, R., Fleck, C., Speck, T., & Bührig-Polaczek, A. (2010). Pummelos as Concept Generators for Biomimetically-Inspired Low Weight Structures with Excellent Damping Properties. *Advanced Engineering Materials*, 12(12), 658-663.

[12] Lacy, A. M., Mora, A., & Boonsiri, I. (1985). Incidence of bubbles on samples cast in a phosphate-bonded investment. *Journal of Prosthetic Dentistry*, 54(3), 367-369.

[13] Chandler, H. T., Fisher, W. T., Brudvik, J. S., & Bottiger, G. (1973). Vacuum-air pressure investing. *Journal of Prosthetic Dentistry*, 29(21), 225-227.

[14] Luk, H. W. K., & Darvell, B. W. (2003). Effect of burnout temperature on strength of gypsum-bonded investments. *Dental Materials*, 19(6), 552-557.

[15] Phillips, R. W. (1947). Relative merits of vacuum investing of small castings as compared to conventional methods. *Journal of Dental Research*, 26(5), 343-352.

[16] Chew, C. L., Land, M. F., Thomas, C. C., & Norman, R. D. (1999). Investment strength as a function of time and temperature. *Journal of Dentistry*, 27(4), 297-302.

[17] Ott, D., & Raub, C. J. (1985). Investment casting of gold jewellery. . Gold Bulletin; , 18(4), 140-143.

[18] O'Brien, W. J., & Nielsen, J. P. (1959). Decomposition of Gypsum Investment in the Presence of Carbon. *Journal of Dental Research*, 38(3), 541-547.

[19] Matsuya, S., & Yamane, M. (1981). Decomposition of Gypsum Bonded Investments. *Journal of Dental Research*, 60(8), 1418-1423.

[20] Luk, H. W. K., & Darvell, B. W. (1997). Effect of burnout temperatures on strength of phosphate-bonded investments- Part II: effect of metal temperature. *Journal of Dentistry*, 25(5), 423-430.

[21] Juszczyk, A. S., Radford, D. R., & Curtis, R. V. (2000). The influence of handling technique on the strength of phosphate-bonded investments. *Dental Materials*, 16(1), 26-32.

[22] Bonilla, W., Masood, S. H., & Iovenitti, P. (2001). An Investigation of Wax Patterns for Accuracy Improvement in Investment Cast Parts. *International Journal of Advanced Manufacturing Technology*, 18(5), 348-356.

[23] Brevick, J. R., Davis, J. W., & Dincher, C. (1991). Towards improving the properties of plaster moulds and castings. *Journal of Engineering Manufacture*, 205(4), 265-269.

[24] Mori, T. (1986). Thermal Behavior of the Gypsum Binder in Dental Casting Investments. *Journal of Dental Research*, 65(6), 877-884.

[25] Gryzlova, E. S., & Kozyreva, N. A. (2009). Displacement of Chemical Equilibria in 12-Salt Six-Component Reciprocal Systems in Melt. *Doklady Chemistry*, 424(1), 19-22.

[26] Eichner, K., & Kappert, H. F. (1995). *Dental materials and their processing*, Stuttgart: Thieme; (in german).

[27] Klein, B. (2007). *Design of experiments-DoE: Introduction to Taguchi/Shainin*, München: Oldenburg Wissenschaftsverlag; (in german).

[28] Kumar, S., Kumar, P., & Shan, H. S. (2008). Optimization of tensile properties of evaporative pattern casting process through Taguchi's method. *Journal of Materials Processing Technology*, 204(1-3), 59-69.

[29] Amathieu, L., & Boistelle, R. (1988). Crystallization Kinetics of Gypsum from dense Suspension of Hemihydrate in Water. *Journal of Crystal Growth*, 88(2), 183-192.

[30] Singh, M., & Garg, M. (1992). Glass Fibre Reinforced Water-Resistant Gypsum-Based Composites. *Cement & Concrete Composites*, 14(1), 23-32.

[31] Klepetsanis, P. G., Dalas, E., & Koutsoukos, P. G. (1999). Role of Temperature in the Spontaneous Precipitation of Calcium Sulfate Dihydrate. *Langmuir*, 15(4), 1534-1540.

[32] Ali, M. A., & Grimer, F. J. (1969). Mechanical Properties of Glass Fibre-Reinforced Gypsum. *Journal of Material Science*, 4(5), 389-395.

[33] Liu, K., Wu, Y. F., & Jiang, X. L. (2008). Shear strength of concrete filled glass fiber reinforced gypsum walls. *Materials Structure*, 41(4), 649-662.

[34] Wertz, S. (1990). Innovative Use of Glass Reinforced Gypsum. *The Construction Specifier*, 43, 76.

[35] Heckl, J., & Krcmar, W. (2006). Improving the stability of gypsum mould by fibre reinforcement. *Ziegelindustrie International- Brick and Tile Industry International*, 59(12), 44-45.

[36] Majumdar & A. J. (1970). Glass Fibre Reinforced Cement and Gypsum Products. *Mathematical Physical and Engineering Science*, 319(1536), 69-78.

[37] Majumdar & A. J. (1974). The role of the interface in glass fibre reinforced cement. *Cement and Concrete Research*, 4(2), 247-266.

[38] Yamagata, H., Kasprzak, W., Aniolek, M., Kurita, H., & Sokolowski, J. H. (2008). The effect of average cooling rates on the microstructure of the Al-20% Si high pressure die casting alloy used for monolithic cylinder blocks. *Journal of Materials Processing Technology*, 203(1-3), 333-341.

[39] Borreguero, A. M., Carmona, M., Sanchez, M. L., Valverde, J. L., & Rodriguez, J. F. (2010). Improvement of the thermal behaviour of gypsum blocks by the incorporatio-nof microcapsules containing PCMS obtained by suspension polymerization with an optimal core/coating mass ratio. *Applied Thermal Engineering*, 30, 1164-1169.

[40] Engler, S. (1972). Solidification morphology and casting properties. *International Journal of Materials Research*, 63(7), 375-379, (in german).

[41] Mabie, C. P. (1973). Petrographic Study of the Refractory Performance of High-Fusing Dental Alloy Investments: I. High-Fired, Phosphate-Bonded Investments. *Journal of Dental Research*, 52(1), 96-110.